

The role of carbon on the electrical properties of polycrystalline $\text{Si}_{1-y}\text{C}_y$ and $\text{Si}_{0.82-y}\text{Ge}_{0.18}\text{C}_y$ films

I. M. Anteney, G. J. Parker, P. Ashburn, and H. A. Kemhadjian
*Department of Electronics and Computer Science, University of Southampton,
 Southampton, SO17 1BJ, England*

(Received 2 August 2000; accepted for publication 1 December 2000)

A comparison is made of the electrical effects of carbon in *n*- and *p*-type *in situ* doped polycrystalline $\text{Si}_{1-y}\text{C}_y$ and $\text{Si}_{0.82-y}\text{Ge}_{0.18}\text{C}_y$ layers. Values of resistivity as a function of temperature, effective carrier concentration and Hall mobility are reported. The *n*-type polycrystalline $\text{Si}_{1-y}\text{C}_y$ and $\text{Si}_{0.82-y}\text{Ge}_{0.18}\text{C}_y$ films show dramatic increases in resistivity with carbon content, rising from 0.044 $\Omega\text{ cm}$ to 450 $\Omega\text{ cm}$ (0 and 0.8% C) and 0.01 $\Omega\text{ cm}$ to 2.4 $\Omega\text{ cm}$ (0 and 0.6% C), respectively. In contrast, the increase in B-doped films is much less severe, rising from 0.001 $\Omega\text{ cm}$ to 0.939 $\Omega\text{ cm}$ (0 and 7.9% C) and 0.003 $\Omega\text{ cm}$ to 0.015 $\Omega\text{ cm}$ (0 and 4% C) for the $\text{Si}_{1-y}\text{C}_y$ and $\text{Si}_{0.82-y}\text{Ge}_{0.18}\text{C}_y$ layers, respectively. The grain boundary energy barrier, determined from the temperature dependence of the resistivity, is found to vary as the square of the C content in the *n*-type polycrystalline $\text{Si}_{1-y}\text{C}_y$ and $\text{Si}_{0.82-y}\text{Ge}_{0.18}\text{C}_y$ layers, but linearly in the *p*-type $\text{Si}_{1-y}\text{C}_y$ layers. The square law dependence seen in the *n*-type layers for C contents up to 0.9% is explained by an increase in the grain boundary trap density due to the presence of carbon, whereas the linear relationship seen in the *p*-type layers for C contents between 2% and 8% is explained by a shift in the grain boundary trap energy toward the valence band. Finally, lower values of grain boundary energy barrier are obtained in *p*-type $\text{Si}_{0.82-y}\text{Ge}_{0.18}\text{C}_y$ layers with a C content of 4% than in equivalent $\text{Si}_{1-y}\text{C}_y$ layers, which could be explained by a larger shift in trap energy toward the valence band. © 2001 American Institute of Physics. [DOI: 10.1063/1.1343896]

INTRODUCTION

For many years, polycrystalline silicon has been a major contributor to the success of silicon integrated circuit technology in applications such as gates for MOS transistors¹ and as polycrystalline emitters for bipolar transistors.² More recently, considerable interest has been shown in polycrystalline SiGe films³⁻⁷ because of their increased dopant activation⁸⁻¹⁰ and lower thermal growth budget. In MOS transistors, polycrystalline SiGe gates could be used to reduce gate depletion and to tailor the work function by varying the Ge content, allowing more freedom in the setting of threshold voltages. Furthermore, these films can be realized using a process that is fully compatible with existing silicon-based technologies. The effects of adding germanium to polycrystalline silicon films differ depending on the type of dopant used. In *p*-type polycrystalline SiGe, the resistivity decreases with increasing Ge content, which has been attributed to increases in both hole mobility and dopant activation with increasing Ge incorporation.^{9,11} In contrast, it has been shown⁹ that for *n*-type films containing less than 25% Ge, the Hall mobility increases, but the effective carrier concentration steadily decreases, with increasing Ge content. The net effect is a slight decrease in the resistivity at low Ge concentrations. For layers with Ge concentrations above 25%, a large drop in phosphorus activation combined with a drop in the Hall mobility is observed,^{4,9} causing a large increase in resistivity. This was attributed to increased phosphorus segregation to the grain boundaries with increasing Ge content.⁹

Polycrystalline $\text{Si}_{1-x-y}\text{Ge}_x\text{C}_y$ and $\text{Si}_{1-y}\text{C}_y$ layers are of interest because they offer the possibility of an additional degree of freedom in band gap engineering not offered by $\text{Si}_{1-x}\text{Ge}_x$ alone. A possible application for polycrystalline $\text{Si}_{1-x-y}\text{Ge}_x\text{C}_y$ and $\text{Si}_{1-y}\text{C}_y$ layers would be as wide band gap emitters for bipolar transistors. Eberl *et al.*¹² have examined the effects of carbon incorporation in single crystal Si and SiGe layers using photoluminescence (PL) measurements on $\text{Si}_{1-y}\text{C}_y$ and $\text{Si}_{1-x-y}\text{Ge}_x\text{C}_y$ quantum well structures. From an extrapolation of the PL results, it was found that for small C concentrations ($\leq 7\%$) the band gap in the $\text{Si}_{1-x-y}\text{Ge}_x\text{C}_y$ layer was increased by 24 meV/% C, whereas the band gap in the $\text{Si}_{1-y}\text{C}_y$ layers was reduced by 65 meV/% C. Amour *et al.*¹³ examined the effect of carbon on both unstrained and strained $\text{Si}_{1-x-y}\text{Ge}_x\text{C}_y$ single crystal layers and found very different behaviors. In strained pseudomorphic layers, the band gap was found to increase by approximately 24 meV/% C, in agreement with Eberl *et al.*, whereas for the unstrained layers, the band gap actually reduced by 10–20 meV/% C for small C concentrations.

Although there is a large body of work on single-crystal $\text{Si}_{1-y}\text{C}_y$ and $\text{Si}_{1-x-y}\text{Ge}_x\text{C}_y$ films, little research has been published on the properties of polycrystalline films. In a previous paper,¹⁴ preliminary results of resistivity, Hall mobility and effective carrier concentration measurements on polycrystalline $\text{Si}_{0.82-y}\text{Ge}_{0.18}\text{C}_y$ films were reported for the first time. In this paper a comparison is made of the electrical properties of polycrystalline $\text{Si}_{1-y}\text{C}_y$ and $\text{Si}_{0.82-y}\text{Ge}_{0.18}\text{C}_y$ layers as a function of carbon content. Measurements of resistivity, Hall mobility and effective carrier concentration on

n- and *p*-type layers are complemented by measurements of the temperature dependence of the resistivity. From these measurements, the grain boundary energy barriers of the layers are extracted, as a function of C content, and used to explain the role of carbon on the measured electrical properties.

EXPERIMENT

In situ doped *p*- and *n*-type amorphous $\text{Si}_{1-y}\text{C}_y$ and $\text{Si}_{0.82-y}\text{Ge}_{0.18}\text{C}_y$ layers were deposited by low pressure chemical vapor deposition (LPCVD) at 500 °C or 540 °C on oxide covered, (100) silicon wafers. The deposition gases were Si_2H_6 , GeH_4 and SiCH_4 for the Si, Ge and C sources, respectively. The *in situ* dopant was introduced during growth using PH_3 or B_2H_6 gases for the *n*- and *p*-type sources, respectively. In all cases, the growth pressure was maintained at 4 Torr and the growth time adjusted to give film thicknesses of approximately 0.6 μm . Following deposition, the layers were capped with 200 nm of deposited oxide and then annealed at 1000 °C for 30 s. This anneal converts the amorphous films into a polycrystalline material and activates the dopant introduced during growth. The oxide cap was then removed and van der Pauw structures defined for Hall measurements. The resistivity, Hall mobility and effective carrier concentration were measured using the van der Pauw structures with an applied magnetic field of 0.2 T. In addition, the temperature dependence of the resistivity was also measured in the range 300 K to 475 K, giving an Arrhenius plot whose slope is equivalent to the activation energy of the resistivity. From this activation energy, the grain boundary energy barrier can be calculated using Eq. (1), where Ψ is given by $1.5 \times 10^{-3}/\text{K}$ and accounts for the shift in the Fermi level with temperature:¹⁵

$$E_a = E_B(1 + \Psi T). \quad (1)$$

Uniform doping profiles were achieved for all *n*- and *p*-type layers, as measured by secondary-ion-mass spectroscopy (SIMS) analysis, and remained largely unaffected by methylsilane flow rate. Average doping concentrations in the polycrystalline $\text{Si}_{1-y}\text{C}_y$ layers were $1.2 \times 10^{19} \text{ cm}^{-3}$ and $7 \times 10^{20} \text{ cm}^{-3}$ for the phosphorus and boron doped layers, respectively. Corresponding doping levels obtained for the *n*- and *p*-type polycrystalline $\text{Si}_{0.82-y}\text{Ge}_{0.18}\text{C}_y$ layers were $4.2 \times 10^{19} \text{ cm}^{-3}$ and $2 \times 10^{20} \text{ cm}^{-3}$. In addition, SIMS measurements of the carbon concentrations in all of the layers showed that the profiles were uniform but that C incorporation in both the *p*-type $\text{Si}_{1-y}\text{C}_y$ and $\text{Si}_{0.82-y}\text{Ge}_{0.18}\text{C}_y$ layers was consistently higher than in the *n*-type layers. A methylsilane flow rate of 10 sccm resulted in a carbon concentration of 1.8% for phosphorus and 7.9% for boron doped polycrystalline $\text{Si}_{1-y}\text{C}_y$ layers. Corresponding carbon concentrations for the phosphorus and boron doped polycrystalline $\text{Si}_{0.82-y}\text{Ge}_{0.18}\text{C}_y$ layers were 1.5% and 4%, respectively. Cross-sectional transmission electron microscopy (TEM) showed that the layers were polycrystalline at the end of processing, with an average grain size of approximately 200 nm.

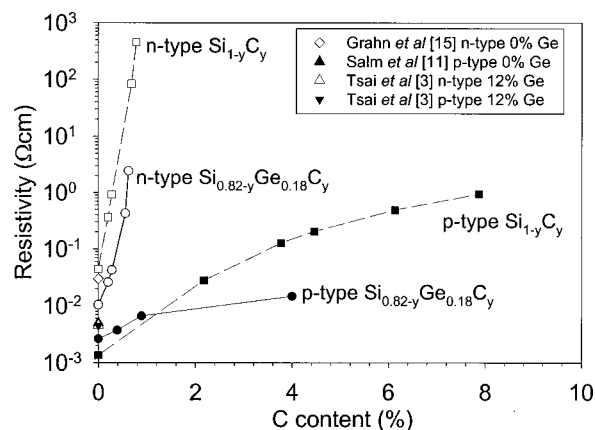


FIG. 1. Graph of layer resistivity versus carbon content for the *n*- and *p*-type polycrystalline $\text{Si}_{1-y}\text{C}_y$ and $\text{Si}_{0.82-y}\text{Ge}_{0.18}\text{C}_y$ layers.

ELECTRICAL RESULTS

The resistivities of the *n*- and *p*-type polycrystalline $\text{Si}_{1-y}\text{C}_y$ and $\text{Si}_{0.82-y}\text{Ge}_{0.18}\text{C}_y$ films, as a function of carbon content, are shown in Fig. 1. For the *n*-type $\text{Si}_{1-y}\text{C}_y$ films, there is a dramatic increase in resistivity with C content, from a value of 0.044 $\Omega \text{ cm}$ with no carbon added, to 450 $\Omega \text{ cm}$ for a C concentration of 0.8%. Not shown in Fig. 1 is the *n*-type layer grown with a C concentration of 1.8%, since the layer was too highly resistive to obtain an experimental value. The *p*-type $\text{Si}_{1-y}\text{C}_y$ films show a much less severe increase in resistivity with carbon content, with resistivity values of 0.001 $\Omega \text{ cm}$ and 0.939 $\Omega \text{ cm}$ for the 0% and 7.9% C concentrations, respectively. A similar trend is also observed in the polycrystalline $\text{Si}_{0.82-y}\text{Ge}_{0.18}\text{C}_y$ layers, though the increase in resistivity of the *p*-type $\text{Si}_{0.82-y}\text{Ge}_{0.18}\text{C}_y$ layers is lower than that for their $\text{Si}_{1-y}\text{C}_y$ counterparts. Also shown in Fig. 1 are resistivity values of polycrystalline Si and SiGe (without carbon) taken from the literature. The layers of Tsai *et al.*³ and Salm *et al.*¹¹ were doped using high dose P^+ (B^+) ion implantation and annealed at 30(3) h at 600 °C and 30(5) min at 950 °C, respectively. In spite of the widely different processing schedules, the values of resistivity are of the same order as those in the current work. The layers of Grahn *et al.*¹⁶ were doped *in situ* with phosphorus and annealed at 1050 °C for 10 s. These processing conditions are very similar to those used in the current work and gave a resistivity value of 0.1 $\Omega \text{ cm}$ for a doping level of $3 \times 10^{19} \text{ cm}^{-3}$. This compares to a value of 0.044 $\Omega \text{ cm}$ for a doping level of $1.2 \times 10^{19} \text{ cm}^{-3}$ in this work. These results show that the layers without carbon in this work are very similar to those reported in the literature.

Figure 2 shows plots of effective carrier concentration versus carbon content for the poly $\text{Si}_{1-y}\text{C}_y$ and poly $\text{Si}_{0.82-y}\text{Ge}_{0.18}\text{C}_y$ layers. From Fig. 2 it can be seen that the effective carrier concentration in the *n*-type poly $\text{Si}_{1-y}\text{C}_y$ layer decreases rapidly with C content, falling from $7.8 \times 10^{18} \text{ cm}^{-3}$ with no carbon added to $2.48 \times 10^{18} \text{ cm}^{-3}$ with the addition of 0.28% C. No experimental value was obtainable for the *n*-type layers with $\geq 0.68\%$ C due to their high resistivity. In contrast, for the *p*-type layers, the effect of C incorporation is much less severe. The effective carrier con-

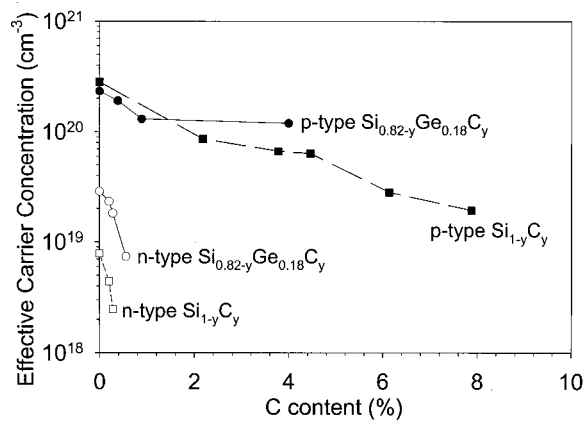


FIG. 2. Graph of effective carrier concentration versus carbon content for the *n*- and *p*-type polycrystalline Si_{1-y}C_y and Si_{0.82-y}Ge_{0.18}C_y layers.

centration is $2.8 \times 10^{20} \text{ cm}^{-3}$ with no C, and falls by approximately an order of magnitude with the addition of 7.9% C. A similar trend is also observed in the polycrystalline Si_{0.82-y}Ge_{0.18}C_y layers, though in this case the drop in effective carrier concentration with C content in the *p*-type layers is less severe for the Si_{0.82-y}Ge_{0.18}C_y layers than for their Si_{1-y}C_y counterparts. Furthermore, the rate of decrease in the effective carrier concentration for the *p*-type Si_{0.82-y}Ge_{0.18}C_y layers is significantly different for C contents above and below 0.9%, suggesting that different mechanisms may be influencing the effective carrier concentration at low and high C concentrations.

Figures 3(a) and 3(b) show plots of the Hall mobility for the polySi_{1-y}C_y and polySi_{0.82-y}Ge_{0.18}C_y layers, respectively. From Fig. 3(a), it can be seen that the Hall mobility in the *n*-type layers dramatically decreases with C content, dropping from a value of 18 cm²/V s with no carbon, to a value of 3 cm²/V s with 0.3% C. In contrast, for the *p*-type layers, the Hall mobility drops much more slowly with C content. The decrease is relatively rapid up to $\approx 4.5\%$ C and then slower for higher C concentrations. The polySi_{0.82-y}Ge_{0.18}C_y layers presented in Fig. 3(b) show a similar trend, though the rate of decrease in the mobility with C content is lower for the *p*-type polycrystalline Si_{0.82-y}Ge_{0.18}C_y layers than for their polySi_{1-y}C_y counterparts. In the Si_{0.82-y}Ge_{0.18}C_y layers, the mobility drops from 10 cm²/V s with no C, to 3.5 cm²/V s with 4% C, compared with 18 cm²/V s to 0.5 cm²/V s for the Si_{1-y}C_y layers containing 0 and 7.8% C.

Figures 4(a) and 4(b) show plots of the log of the normalized sheet resistance versus $1/kT$ for the *n*- and *p*-type polycrystalline Si_{1-y}C_y layers, respectively, for different C contents. For the *n*-type layers, it can be seen that the addition of C causes a significant increase in the activation energy E_A , from a value of 46 meV with no carbon, to 390 meV with the addition of 0.78% C. In contrast, for the *p*-type layers, the increase in activation energy E_a with C content is much smaller, even though the C content is significantly larger. The activation energy rises from a value of 16 meV with 2.2% C to 75 meV with 7.9% C. The activation energy for the *p*-type layer containing no carbon could not be ex-

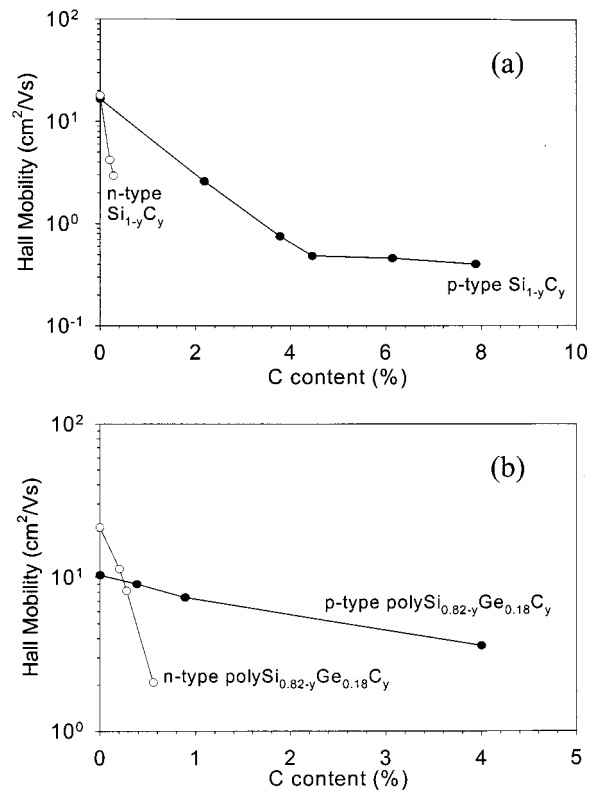


FIG. 3. Graph of Hall mobility versus carbon content for (a) *n*- and *p*-type polycrystalline polySi_{1-y}C_y layers and (b) *n*- and *p*-type polycrystalline Si_{0.82-y}Ge_{0.18}C_y layers.

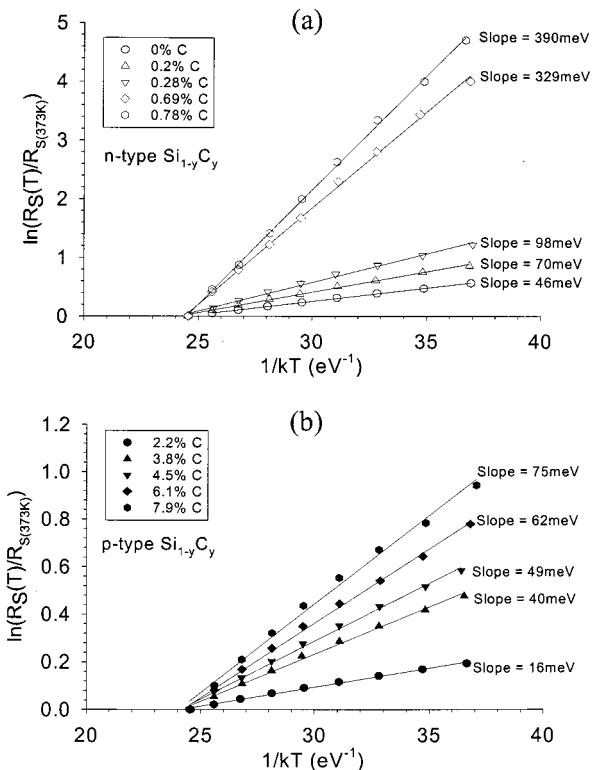


FIG. 4. Logarithm of the normalized sheet resistance versus $1/kT$ for (a) *n*-type polycrystalline polySi_{1-y}C_y layers and (b) *p*-type polycrystalline polySi_{1-y}C_y layers.

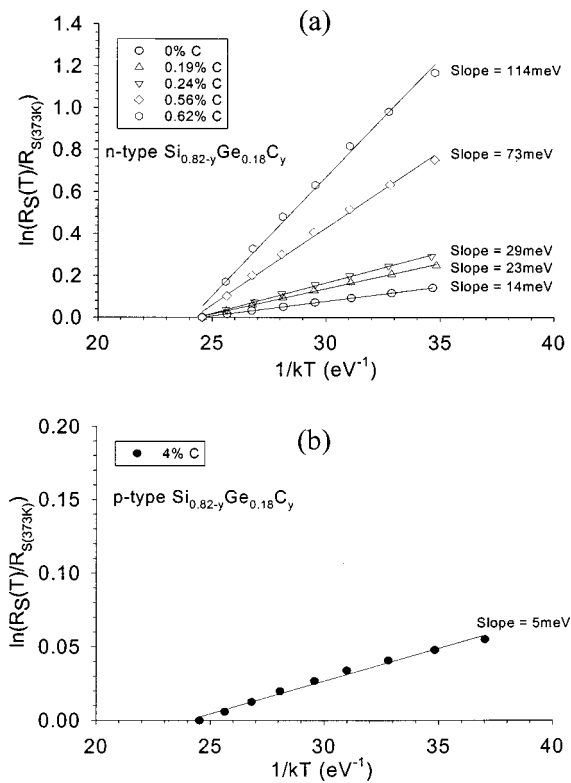


FIG. 5. Logarithm of the normalized sheet resistance versus $1/kT$ for (a) n -type polycrystalline $\text{Si}_{0.82-y}\text{Ge}_{0.18}\text{C}_y$ layers and (b) p -type polycrystalline $\text{Si}_{0.82-y}\text{Ge}_{0.18}\text{C}_y$ layers.

tracted because the grain boundary energy barrier was too small, indicating that conduction is not thermally activated and is limited by some other mechanism such as ionized impurity scattering.

Figures 5(a) and 5(b) show plots of the log of the normalized sheet resistance versus $1/kT$ for the n - and p -type poly $\text{Si}_{0.82-y}\text{Ge}_{0.18}\text{C}_y$ layers, respectively. For the n -type layers, a similar trend is observed to that found in the poly $\text{Si}_{1-y}\text{C}_y$ layers, with the activation energy rising from 14 meV with no C added, to 114 meV with 0.62% C. For the p -type layers, the activation energy could only be extracted for the layer containing the highest C content (4%), indicating that conduction in the other layers was not thermally activated and hence not limited by the grain boundary energy barrier. Even at this high C content, the extracted activation energy is only 5 meV, compared to a value of 45 meV for the poly $\text{Si}_{1-y}\text{C}_y$ layer with a similar C content and a factor of 3.3 higher doping level.

DISCUSSION

The above results indicate that the effect of carbon on the electrical properties of the polycrystalline $\text{Si}_{1-y}\text{C}_y$ and $\text{Si}_{0.28-y}\text{Ge}_{0.18}\text{C}_y$ layers is significantly different in n - and p -type layers. In n -type (P doped) layers, the resistivity dramatically increases with C concentration, whereas in p -type (B doped) layers the increase in resistivity is much smaller. To give insight into this behavior, the model for conduction in polycrystalline Si will first be considered.

In polycrystalline silicon, defects at the grain boundaries introduce trapping centers into the energy gap, immobilizing the free carriers from substitutional dopant atoms and causing the defects to become electrically charged.¹⁷ This gives rise to a potential energy barrier that impedes the flow of carriers from one crystallite to another, thus limiting conduction. Similar behavior is exhibited by n - and p -type polycrystalline silicon layers indicating that either type of majority carrier can be trapped at the grain boundaries, and that the grain boundary traps are located near the middle of the energy gap. Seager¹⁸ has reported that the dominant trap energy level in polycrystalline silicon is located slightly below mid-gap at an energy level of approximately $E_C - 0.62$ eV. This is close to the energy level reported for the silicon dangling bond which is located at $E_C - 0.65$ eV.¹⁹ At high dopant concentrations, the grain boundary traps become fully occupied, allowing any additional free carriers to form a neutral region within the crystallite, reducing the depletion regions at the grain boundaries and lowering the potential barrier.^{17,20} For a highly doped layer, where a depletion region exists within the grain and the grain boundary trap energy level is fixed (close to the middle of the band gap), the grain boundary energy barrier E_B is given by:¹⁷

$$E_B = \frac{q^2 N_T^2}{8 \epsilon N}, \quad (2)$$

where N_T is the grain boundary trap density, ϵ is the relative permittivity of the layer, N is the dopant level and q is the charge on an electron.

Although the grain boundary barriers are similar for n - and p -type polycrystalline silicon layers, dopant segregation can lead to differences in electrical behavior. Mandurah *et al.*²¹ have shown that As and P segregate to grain boundaries whereas B does not. This can cause differences in conduction since segregated dopant is electrically inactive and hence cannot reduce the grain boundary energy barrier. Other mechanisms that could influence the resistivity of the layers are silicon carbide precipitation and substitutional carbon in the grains. Silicon carbide precipitation in single crystal $\text{Si}_{1-y}\text{C}_y$ is a well known phenomenon but in order to explain the resistivity results in this work, the precipitation would have to be considerably worse in the low C content n -type layers than in the high C content p -type layers. This is highly unlikely. The effects of substitutional carbon would be expected to influence the mobility through alloy scattering. However, this effect should be small and would again be expected to be worse in the high C content p -type layers than in the low C content n -type layers.

To gain further insight into the mechanism controlling the resistivity, the measured grain boundary energy barrier versus carbon content at 300 K for the n -type polycrystalline $\text{Si}_{1-y}\text{C}_y$ and $\text{Si}_{0.82-y}\text{Ge}_{0.18}\text{C}_y$ layers has been plotted in Fig. 6(a). From Fig. 6(a) it can be seen that the grain boundary energy barriers in the polycrystalline $\text{Si}_{1-y}\text{C}_y$ are larger, for a given C content, than in their polycrystalline $\text{Si}_{0.82-y}\text{Ge}_{0.18}\text{C}_y$ counterparts. A possible explanation for this difference could be differences in doping level [see Eq. (2)], since the average doping levels in the $\text{Si}_{1-y}\text{C}_y$ and $\text{Si}_{0.82}\text{Ge}_{0.18}\text{C}_y$ layers were $1.2 \times 10^{19} \text{ cm}^{-3}$ and 4.2

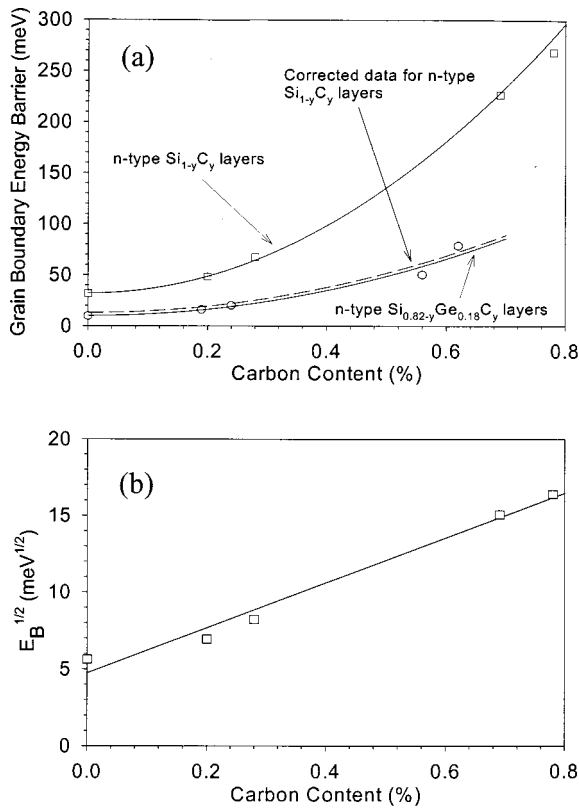


FIG. 6. (a) Plot of the grain boundary energy barrier E_B vs C content for the n -type polycrystalline polySi_{1-y}C_y and polySi_{0.82-y}Ge_{0.18}C_y layers. (b) Plot of $\sqrt{E_B}$ vs C content for the n -type polySi_{1-y}C_y layers.

$\times 10^{19} \text{ cm}^{-3}$, respectively. To investigate whether this is the case, Eq. (2) was used to correct the measured polycrystalline Si_{1-y}C_y energy barriers to a doping level of $4.2 \times 10^{19} \text{ cm}^{-3}$, equivalent to that found in the polycrystalline Si_{0.82-y}Ge_{0.18}C_y layers. The results of this correction are also shown in Fig. 6(a) as the dashed line, where it can be seen that the corrected data coincide very well with the measured data for the polySi_{0.82-y}Ge_{0.18}C_y layers. This result shows that the different values of grain boundary energy barrier in n -type polycrystalline Si_{1-y}C_y and Si_{0.82-y}Ge_{0.18}C_y layers are entirely attributable to differences in doping level. Furthermore, it can be inferred from this result that Ge in the n -type Si_{0.82-y}Ge_{0.18}C_y layers has a negligible effect on the resistivity for C contents up to 0.6%. Figure 6(b) shows a graph of the square root of the grain boundary energy barrier as a function of C content. The data fall on a reasonably good straight line, indicating that the energy barrier varies as the square of the carbon content. This square law dependence is fully consistent with Eq. (2) and suggests that at low C concentrations up to 0.8%, the carbon is increasing the trap density N_T at the grain boundaries.

Figure 7 shows a plot of the measured grain boundary energy barrier versus C content at 300 K for the p -type polycrystalline polySi_{1-y}C_y layers. The relationship between the grain boundary energy barrier E_B and C content for the p -type layers can be reasonably approximated by a linear fit. This contrasts with the square law fit found in the n -type Si_{1-y}C_y layers, suggesting that the mechanism controlling the resis-

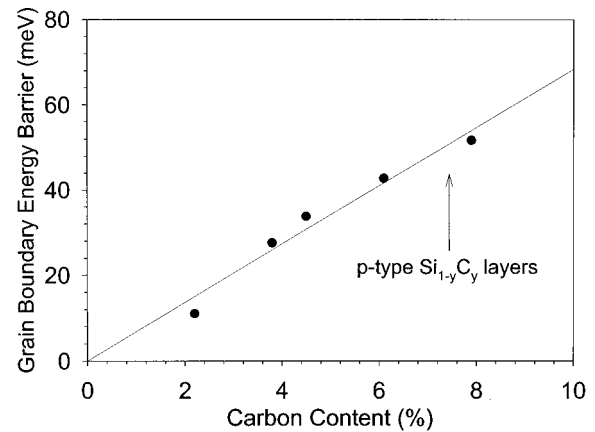


FIG. 7. Plot of the grain boundary energy barrier versus C content for the p -type polycrystalline polySi_{1-y}C_y layers.

tivity in the high C content p -type layers is different than that in the low C content n -type layers. No experimental data are available for p -type Si_{1-y}C_y layers at low C contents ($\leq 1\%$). However, it is possible to replot the n -type Si_{1-y}C_y data corrected to a doping level of $7 \times 10^{20} \text{ cm}^{-3}$, equivalent to that found in the p -type layers. This is shown in Fig. 8 and indicates that the data for the low C content n -type layers lie close to the line for the high C content p -type layers. This result suggests that low C content p -type polycrystalline Si_{1-y}C_y layers might behave in a similar way to the low C content n -type layers.

The behavior of p -type Si_{1-y}C_y layers at higher C contents cannot be explained solely by an increase in the grain boundary trap density (N_T) with C content, as shown in Fig. 8. The predicted curve represents the grain boundary energy barrier that has been calculated using Eq. (2), assuming that the barrier height is determined solely by N_T . The predicted grain boundary trap density was calculated by extrapolating the relationship between N_T and C content, obtained for the n -type layers, to the higher C concentrations found in the p -type layers. While agreement with theory is reasonable for

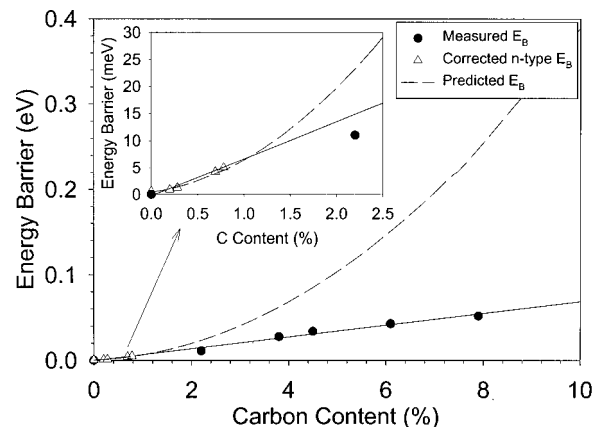


FIG. 8. Comparison between the predicted and measured E_B for the p -type polySi_{1-y}C_y layers. The predicted energy barriers were calculated using the trap density/C content relationship in the n -type layers. In the calculations it is assumed that the energy barrier is solely determined by the grain boundary trap density.

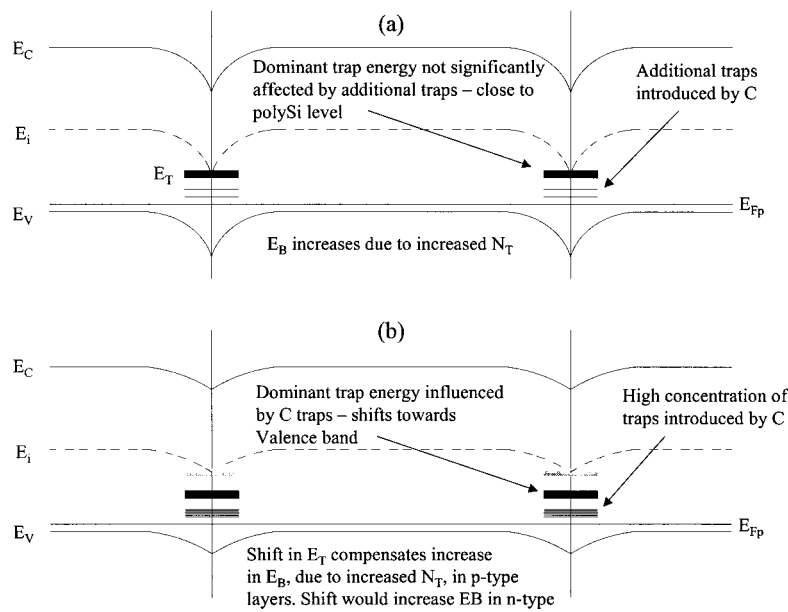


FIG. 9. Schematic diagram of the energy bands in p -type $\text{polySi}_{1-y}\text{C}_y$ showing how the shift in $E_F - E_T$, relative to the polycrystalline Si case, reduces the grain boundary energy barrier for a given N_T .

C contents up to 1%, at higher C contents there is a large discrepancy between the predicted and measured data. This result clearly shows that Eq. (2) is not valid for C concentrations above 1%.

Equation (2) assumes that the grain boundary trap energy is not influenced by the carbon content. However, there is some evidence in the literature to suggest that the trap energy in polycrystalline materials can shift at high impurity contents. Several authors have shown that the addition of $\geq 25\%$ Ge to polycrystalline $\text{Si}_{1-x}\text{Ge}_x$ layers causes a significant increase in resistivity of n -type layers, and a corresponding decrease in p -type layers.⁹⁻¹¹ In polycrystalline Si, the dominant trap energy is close to the middle of the band gap, so that the effects of the carrier trapping are similar in both n - and p -type layers. In polycrystalline Ge, the dominant trap energy is close to the valence band, so that grain boundary energy barriers only appear in n -type material.²² It is therefore believed,¹¹ that the addition of Ge to form polycrystalline $\text{Si}_{1-x}\text{Ge}_x$ causes a progressive shift in the dominant trap energy toward the valence band. At high Ge concentrations ($x \geq 0.25$) the shift in trap energy results in a lowering of the potential barrier for p -type layers and an increase for n -type, thereby explaining the corresponding decrease and increase in the resistivities of the layers.

Londos²³ showed, by deep level transient spectroscopy, that interstitial carbon introduces a deep level donor defect into the band gap ($E_V + 0.28$ eV) of single-crystal silicon. It is therefore possible that carbon trapped at grain boundaries in polycrystalline $\text{Si}_{1-y}\text{C}_y$ could introduce such a defect in the energy gap. If this was the case, as more carbon was added, the number of traps located at or near $E_V + 0.28$ eV would increase and begin to influence the dominant trap energy in the grain boundary, shifting it toward the valence band. Figure 9 schematically illustrates the effect of the trap energy on the grain boundary energy barrier in p -type material. As the trap energy shifts from mid-gap [Fig. 9(a)] toward the valence band [Fig. 9(b)], the grain boundary energy barrier is reduced, thereby partially compensating the in-

crease in energy barrier associated with the increase in N_T due to C. This would explain the large difference between the predicted and measured grain boundary energy barriers seen for the p -type polycrystalline $\text{Si}_{1-y}\text{C}_y$ layers in Fig. 8. In contrast, it can be expected that for n -type layers with high C contents, the shift in E_T would increase the energy barrier and therefore add to the increase associated with the increased trap density.

An extension to the simple carrier trapping model has been proposed by Baccarani *et al.*²⁴ which takes into account the effects of the movement of the trap energy level E_T on the grain boundary energy barrier. If the effect of increasing the density of the traps (N_T) per unit area, located at a discrete energy level E_T is considered, the equation describing the grain boundary energy barrier becomes:

$$E_B \approx \frac{1}{2} E_G - E_T + kT \ln \left[\frac{qN_T \sqrt{N}}{N_V \sqrt{2\epsilon E_B}} \right], \quad (3)$$

which can be solved iteratively for a given N_T , E_T and N . For the p -type layers in this work, the grain boundary energy barrier E_B and the effective carrier concentration N have been measured. In addition, values for the grain boundary trap density N_T can be obtained for the higher C contents by extrapolating the data for the low C content n -type layers. Equation (3) can then be used to calculate values of E_T as a function of C content for the p -type layers, as shown in Fig. 10. The band gap of silicon ($E_G = 1.12$ eV) was used in the calculations because of the uncertainty in the amount of substitutional carbon within the grains of the $\text{Si}_{1-y}\text{C}_y$ samples. A large shift in trap energy is predicted from ≈ 0.5 eV for polycrystalline silicon¹⁸ to 0.41 eV for 2% C and 0.38 eV for 7.9% C. These results suggest that the effect of C on the resistivity of the p -type $\text{polySi}_{1-y}\text{C}_y$ layers can be explained if high concentrations of carbon affect not only the grain boundary trap density, but also shift the trap energy level toward the valence band.

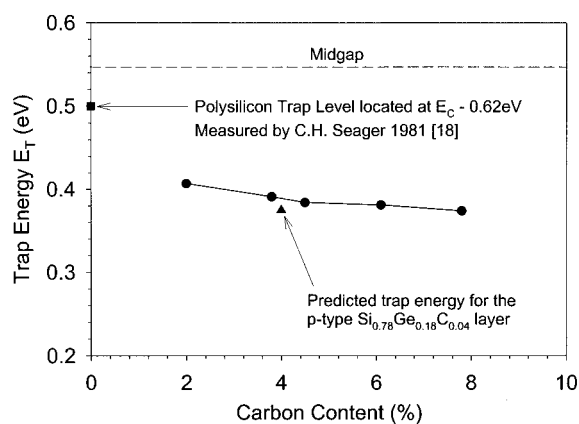


FIG. 10. Graph of grain boundary trap energy E_T versus carbon content for the p -type polycrystalline $\text{Si}_{1-y}\text{C}_y$ layers, showing how the trap energy level shifts away from the grain boundary Fermi level toward the valence band.

For the p -type polycrystalline $\text{Si}_{0.82-y}\text{Ge}_{0.18}\text{C}_y$ layers, a grain boundary energy barrier of 3.5 meV was obtained for the layer containing 4% C. This is over a factor of 9 lower than the corresponding energy barrier for the polycrystalline $\text{Si}_{1-y}\text{C}_y$ layer with a similar C content. This discrepancy cannot be explained by a difference in doping level because the boron concentration in the polycrystalline $\text{Si}_{0.78}\text{Ge}_{0.18}\text{C}_{0.04}$ layer was a factor of 3.5 lower than its $\text{Si}_{0.962}\text{C}_{0.038}$ counterpart. A correction for this difference would make the discrepancy even bigger. This result therefore indicates that the incorporation of 18% Ge in the high C content p -type layers is counteracting the effects of carbon in some way. In contrast, the incorporation of 18% Ge into the low C content n -type layers has no significant effect.

The result shown in Fig. 10 for the p -type polycrystalline $\text{Si}_{0.78}\text{Ge}_{0.18}\text{C}_{0.04}$ layer indicates that there is a larger shift in the grain boundary trap energy level toward the valence band than in the p -type $\text{Si}_{1-y}\text{C}_y$ layer with a similar C content. This could explain the lower values of grain boundary energy barrier obtained for the $\text{Si}_{0.78}\text{Ge}_{0.18}\text{C}_{0.04}$ layer since the larger shift in trap energy level toward the valence band would further compensate the effects of the increasing grain boundary trap density with C content. Additional mechanisms that could also partially account for the reduced grain boundary energy barrier in the p -type $\text{Si}_{0.78}\text{Ge}_{0.18}\text{C}_{0.04}$ layer are increased boron activation and larger grain size with increasing Ge content. However, this hypothesis is based on very limited experimental data and so further work is required to study the effects of Ge content on the behavior of p - and n -type polycrystalline $\text{Si}_{1-x-y}\text{Ge}_x\text{C}_y$ layers.

Finally, it should be noted that although the methylsilane flow rates were kept constant to allow direct comparisons between successive growth runs, SIMS analysis has shown that the carbon incorporation in the p -type layers was consistently higher than in their n -type counterparts. Maximum carbon contents of 7.9% and 4% were obtained for the p -type poly $\text{Si}_{1-y}\text{C}_y$ and poly $\text{Si}_{0.82-y}\text{Ge}_{0.18}\text{C}_y$ layers, respectively, while the corresponding contents obtained for the n -type layers, for the same methylsilane gas flow, were only 1.8% and 1.5%. A possible explanation for these differences

in the carbon content is the effectiveness of phosphine at blocking surface sites for silane chemisorption, thus inhibiting growth.^{25,26} In contrast, diborane does not block the surface sites, and thus allows easier chemisorption of SiH_4 and better growth rates. Since the chemisorption of SiCH_6 is likely to be similar to that of silane, the reduced number of available surface sites could lead to a reduction in the amount of carbon incorporated into the layer. Further work is required to investigate the growth kinetics for the deposition of n - and p -type $\text{Si}_{1-y}\text{C}_y$ and $\text{Si}_{1-x-y}\text{Ge}_x\text{C}_y$ layers.

CONCLUSIONS

A study has been made of the role of carbon on the electrical properties of n - and p -type polycrystalline $\text{Si}_{1-y}\text{C}_y$ and $\text{Si}_{0.82-y}\text{Ge}_{0.18}\text{C}_y$ layers for C contents in the range of 0%–8%. Phosphorus and boron doping levels of $1.2 \times 10^{19} \text{ cm}^{-3}$ and $7 \times 10^{20} \text{ cm}^{-3}$ were achieved for the n - and p -type $\text{Si}_{1-y}\text{C}_y$ layers, respectively, and remained largely unaffected by carbon content. Corresponding doping levels in the $\text{Si}_{0.82-y}\text{Ge}_{0.18}\text{C}_y$ layers were $4 \times 10^{19} \text{ cm}^{-3}$ and $2 \times 10^{20} \text{ cm}^{-3}$.

Electrical measurements have shown that for n -type polycrystalline $\text{Si}_{1-y}\text{C}_y$ and $\text{Si}_{0.82-y}\text{Ge}_{0.18}\text{C}_y$ layers, the addition of a small amount of carbon ($\leq 0.9\%$) causes a severe increase in resistivity. This is accompanied by a corresponding drop in effective carrier concentration and Hall mobility. In contrast, for p -type layers, the effect of C on the resistivity is much less dramatic. Measurements of the grain boundary energy barrier for n -type poly $\text{Si}_{1-y}\text{C}_y$ and poly $\text{Si}_{0.82-y}\text{Ge}_{0.18}\text{C}_y$ layers, extracted from the temperature dependence of the resistivity, have shown that there is a square law dependence on carbon content for C contents up to 0.9%. This result is explained by an increase in the density of traps at the grain boundaries due to the presence of carbon. In contrast, the grain boundary energy barriers in the p -type poly $\text{Si}_{1-y}\text{C}_y$ layers exhibit a linear dependence on carbon content for C contents between 2% and 8%, indicating some other mechanism is involved. This result has been explained by a shift in the dominant trap energy level toward the valence band at high C concentrations. In p -type layers, this shift reduces the energy barrier, therefore compensating the effect of the increasing grain boundary trap density. In n -type layers, the shift in the trap energy at high C concentrations would cause a corresponding increase in the grain boundary energy barrier, adding to the increase associated with the increased trap density.

Finally, it has been shown that a much lower value of grain boundary energy barrier is obtained for a p -type $\text{Si}_{0.78}\text{Ge}_{0.18}\text{C}_{0.04}$ compared to a $\text{Si}_{1-y}\text{C}_y$ layer with a similar C content. Results show that a larger shift in the grain boundary trap energy level toward the valence band is predicted with the inclusion of 18% Ge. This increased shift in trap energy level would give additional compensation to the effects of increased grain boundary trap density with C content, thereby explaining the lower grain boundary energy barrier.

¹T. Yamamoto, K. Uwasawa, and T. Mogamu, IEEE Trans. Electron Devices **46**, 921 (1999).

- ²I. R. C. Post, P. Ashburn, and G. R. Wolstenholme, *IEEE Trans. Electron Devices* **39**, 1717 (1992).
- ³J. Tsai, A. Tang, T. Noguchi, and R. Reif, *J. Electrochem. Soc.* **142**, 3220 (1995).
- ⁴T. J. King and K. Saraswat, *J. Electrochem. Soc.* **141**, 2235 (1994).
- ⁵V. Subramanian and K. Saraswat, *IEEE Trans. Electron Devices* **45**, 1690 (1998).
- ⁶V. Li, M. R. Mirabedini, R. T. Kuehn, J. J. Wortman, M. Ozturk, D. Batchelor, K. Christensen, and D. Maher, *Appl. Phys. Lett.* **71**, 3388 (1997).
- ⁷V. Li, M. R. Mirabedini, B. Hornung, H. Heinisch, M. Xu, D. Batchelor, D. Maher, J. J. Wortman, and R. T. Kuehn, *J. Appl. Phys.* **83**, 5469 (1998).
- ⁸W. Edwards, Y. Chieh, S. Lin, D. Ast, J. Krusius, and T. Kamins, *Mater. Res. Soc. Symp. Proc.* **343**, 685 (1994).
- ⁹D. Bang, M. Cao, A. Wang, K. Saraswat, and T. King, *Appl. Phys. Lett.* **66**, 195 (1997).
- ¹⁰Z. Jin, B. Gururaj, W. Yeung, H. Kwok, and M. Wong, *IEEE Trans. Electron Devices* **44**, 1958 (1997).
- ¹¹C. Salm, D. van Veen, D. Gravesteijn, J. Holleman, and P. Woerlee, *J. Electrochem. Soc.* **144**, 3665 (1997).
- ¹²K. Eberl, K. Brunner, and W. Winter, *Thin Solid Films* **294**, 98 (1997).
- ¹³A. Amour, C. Liu, J. Sturm, Y. Lacroix, and M. Thewalt, *Appl. Phys. Lett.* **67**, 3915 (1995).
- ¹⁴I. M. Anteney, G. J. Parker, P. Ashburn, and H. A. Kemhadjian, *Appl. Phys. Lett.* **77**, 561 (2000).
- ¹⁵H. C. de Graaff, M. Huybers, and J. de Groot, *Solid-State Electron.* **25**, 67 (1982).
- ¹⁶J. V. Grahn, J. Pejnefors, M. Sanden, S. L. Zhang, and M. Ostling, *J. Electrochem. Soc.* **144**, 3952 (1997).
- ¹⁷T. Kamins, *J. Appl. Phys.* **42**, 4357 (1971).
- ¹⁸C. H. Seager, *J. Appl. Phys.* **52**, 3960 (1981).
- ¹⁹W. B. Jackson, N. M. Johnson, and D. K. Biegelsen, *Appl. Phys. Lett.* **43**, 195 (1983).
- ²⁰J. Seto, *J. Appl. Phys.* **46**, 5247 (1975).
- ²¹M. M. Mandurah, K. C. Saraswat, and C. R. Helms, *J. Appl. Phys.* **51**, 5755 (1980).
- ²²T. Kamins (Wiley, New York, 1981).
- ²³C. Londos, *Phys. Rev. B* **35**, 6295 (1987).
- ²⁴G. Baccarani, B. Ricco, and G. Spadini, *J. Appl. Phys.* **49**, 5565 (1978).
- ²⁵B. S. Meyerson and M. L. Yu, *J. Electrochem. Soc.* **131**, 2366 (1984).
- ²⁶M. L. Yu, D. J. Vitkavage, and B. S. Meyerson, *J. Appl. Phys.* **59**, 4032 (1986).